Binding and Cleavage of Nucleic Acids by the "Hairpin" Ribozyme†

Bharat M. Chowrira and John M. Burke*

Department of Microbiology and Molecular Genetics, Markey Center for Molecular Genetics, The University of Vermont, Burlington, Vermont 05405

Received May 31, 1991; Revised Manuscript Received July 8, 1991

ABSTRACT: The "hairpin" ribozyme derived from the minus strand of tobacco ringspot virus satellite RNA [(−)sTRSV] efficiently catalyzes sequence-specific RNA hydrolysis in trans (Feldstein et al., 1989; Hampel & Tritz, 1989; Haseloff & Gerlach, 1989). The ribozyme does not cleave DNA. An RNA substrate analogue containing a single deoxyribonucleotide residue 5′ to the cleavage site (A_{-1}) binds to the ribozyme efficiently but cannot be cleaved. A DNA substrate analogue with a ribonucleotide at A_{-1} is cleaved; thus A_{-1} provides the only 2′-OH required for cleavage. These results support cleavage via a transphosphorylation mechanism initiated by attack of the 2′-OH of A_{-1} on the scissile phosphodiester. The ribozyme discriminates between DNA and RNA in both binding and cleavage. Results indicate that the 2′-OH of A_{-1} functions in complex stabilization as well as cleavage. The ribozyme efficiently cleaves a phosphorothioate diester linkage, suggesting that the *pro*-R_p oxygen at the scissile phosphodiester does not coordinate Mg^{2+}.

Ribozymes (RNA enzymes) catalyze site-specific RNA cleavage and ligation reactions. In contrast to most protein ribonucleases, ribozymes show a high degree of sequence specificity. Since interactions between ribozymes and substrates are RNA–RNA interactions, ribozymes with altered sequence specificities can be generated. This leads to the expectation that engineered ribozymes may serve as useful RNA cleavage tools in vitro and in vivo. Currently we and others are attempting to construct ribozymes that may be useful as gene-specific therapeutic agents. Results of experiments to date suggest that while targeted alterations in sequence-specificity are readily accomplished, they are frequently accompanied by an unacceptable loss of catalytic efficiency (Ruffner et al., 1989; Fedor & Uhlenbeck, 1990; Hampel et al., 1990; S. Joseph and J. Burke, unpublished results). In order to engineer optimally active ribozymes against foreign target sequences, a detailed understanding of the mechanism of substrate binding and cleavage is necessary.

The "hairpin" ribozyme derived from the minus strand of tobacco ringspot virus satellite RNA [(−)sTRSV][1] efficiently cleaves RNA substrates in trans (Feldstein et al., 1989; Hampel & Tritz, 1989; Haseloff & Gerlach, 1989). Substrate binding involves formation of two short intermolecular helices (Hampel et al., 1990; helix 1 and helix 2, Figure 1). Four substrate bases encompassing the cleavage site might be recognized by a mechanism involving tertiary interactions with the ribozyme. Here, we report results of experiments that probe the functional roles of substrate 2′-hydroxyl groups and the *pro*-R_p oxygen at the scissile phosphodiester.

Experimental Procedures

Synthesis of RNA and Mixed RNA/DNA Oligonucleotides. Transcription of synthetic DNA with T7 RNA polymerase was carried out as described (Milligan & Uhlenbeck, 1989). Synthetic substrates and substrate analogues were synthesized by using RNA phosphoramidite chemistry as described (Scaringe et al., 1990), with standard DNA reagents except for RNA phosphoramidites (Milligen). Crude deprotected oligoribonucleotides were 5′-end-labeled and then gel-purified.

Table I: Sequences of Substrates and Substrate Analogues[a]

substrate or analogue	sequence
R	5′ UGACA↓GUCCUGUUU 3′
Rt	5′ GCGUGACA↓GUCCUGUUU 3′
var	5′ GCGUCACA↓GUCCUCUUU 3′
D	5′ UGACA↓GUCCUGUUU 3′
DrA	5′ UGACA↓GUCCUGUUU 3′
DrG	5′ UGACA↓GUCCUGUUU 3′
RdA	5′ UGACA↓GUCCUGUUU 3′

[a] Deoxyribonucleotide residues are underlined. Arrow indicates cleavage site.

Ribozyme Reactions. Reactions contained 18 pmol of ribozyme and 100 pmol of substrate in a standard reaction buffer [2 mM spermidine, 40 mM Tris-HCl (pH 7.5), and $MgCl_2$ concentrations as indicated]. RNAs were renatured by heating the RNAs to 95 °C for 2 min, followed by cooling on ice for 30 min. Reactions were initiated by incubation at 37 °C. Under these conditions, no reaction products were detectable without the 37 °C incubation. Reactions were terminated by addition of 10 μL of loading buffer (containing 8 M urea) and heating to 95 °C for 1 min.

Quantitative analyses of reactions were carried out by radioanalytic imaging of dried gels with a Betascan instrument (Betagen). Kinetic parameters were estimated by curve-fitting with "kcat" software (BioMetallics).

Analysis of Ribozyme–Substrate Complex Formation. Complex formation was assayed by incubating renatured unlabeled ribozyme (15 nM) and ^{32}P-end-labeled substrate or substrate analogue (30 nM) in standard reaction buffer (10 μL). Complexes were allowed to form for 2 h on ice. An equal volume of 50% glycerol was added and samples were loaded

† Supported by grants from the NIH, the Pfieffer Foundation, and the NSF EPSCOR program.

* Corresponding author.

[1] Abbreviations: (−)sTRSV, negative RNA strand of the satellite RNA of tobacco ringspot virus.

0006-2960/91/0430-8518$02.50/0

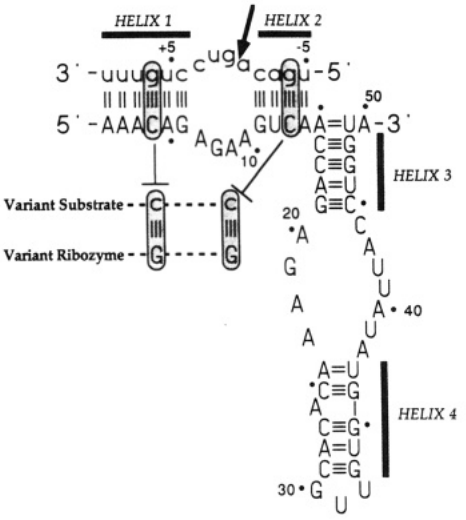

FIGURE 1: Secondary structure of the (−)sTRSV ribozyme–substrate complex. Uppercase, ribozyme sequences; lowercase, substrate sequences. Arrow indicates substrate cleavage site. Evidence for helices 1–4 derives from computer-assisted RNA folding, phylogenetic analysis, analysis of compensatory mutations, and molecular modeling (Hampel & Tritz, 1989; Hampel et al., 1990; Feldstein et al., 1989; Haseloff & Gerlach, 1989; Rubino et al., 1990; data not shown). Shaded nucleotides denote base substitutions in sequence variants.

onto a 15% native polyacrylamide gel, containing 40 mM Tris–acetate (pH 7.5) and 12 mM magnesium acetate. Gels were prepared and run as described (Fedor & Uhlenbeck, 1990).

Results and Discussion

Requirements for Ribose. We asked whether the ribozyme was able to cleave a DNA analogue of the substrate. No cleavage of the oligodeoxyribonucleotide UGACA/GUCCUGUU (designated D, Table I) was observed under any conditions tested (Figure 2 and data not shown; $MgCl_2$ concentrations from 12 to 100 mM, temperatures from 4 to 55 °C, incubation times up to 36 h, and ribozyme:substrate ratios up to 300:1 were tested). In order to determine which ribose moieties were required, we tested activity against a series of mixed DNA/RNA oligonucleotides. The ribozyme was unable to cleave an RNA oligonucleotide with a deoxyadenosine immediately 5′ to the cleavage site (position −1, oligonucleotide RdA). Cleavage of RdA was tested under the same range of conditions described above. A control synthetic all-RNA substrate (oligonucleotide R) was cleaved with kinetics comparable to that of the transcriptionally synthesized control RNA substrate (oligonucleotide Rt, Figure 2).

Inhibition studies showed that RdA is a competitive inhibitor of the ribozyme (K_I = 3.7 ± 1.7 μM). From the observed K_I, we estimate an apparent ΔG of −7.4 kcal/mol for binding of RdA by the ribozyme in cleavage buffer at 37 °C. This value should be considered a very rough estimate, since native gel analysis shows the presence of two conformational isomers of the ribozyme and multiple forms of the inhibitor (Figure 3). In contrast, analogue D is a poor inhibitor of the reaction, showing mixed inhibition only at high concentrations (data not shown). Inhibition by D was not more effective than inhibition by a control DNA oligonucloeotide of unrelated sequence (T7 promoter). These kinetic data show that the ribozyme binds DNA more weakly than RNA; inhibition results from nonspecific binding.

Together, these results clearly indicate that the 2′-hydroxyl stereochemically adjacent to the scissile phosphodiester is essential for the cleavage reaction, and provides strong evidence to support a transphosphorylation mechanism initiated by attack of the 2′-hydroxyl of A_{-1} on phosphorus at the cleavage site (Figure 2D; Van Tol et al., 1990).

Are other 2′-hydroxyl groups required for cleavage? We found that the ribozyme could cut a DNA substrate with riboadenosine at position −1 (oligonucleotide DrA) with low efficiency (Figure 2A,B). Estimation of kinetic parameters revealed that catalytic efficiency (k_{cat}/K_M) for DrA cleavage was lower than that for substrates R by a factor of about 10^5 (Figure 2C). No cleavage of a control oligonucleotide with a single ribose at position +1 (DrG) was observed under any conditions tested. We conclude that ribose is required only at position A_{-1} for cleavage to occur. However, the presence of other ribose moieties is clearly important for optimal cleavage rates. Yang et al. (1990) have shown that a 2′-OH at the cleavage site is required by the hammerhead ribozyme. These results are similar to our results on the hairpin ribozyme. In contrast, the hammerhead cleaves a DNA analogue of the substrate containing a single ribonucleotide residue at the cleavage site much more efficiently than does the hairpin ribozyme.

Binding of Substrate and Noncleavable Analogues. Native gel analysis was used to examine formation of complexes between ribozyme and substrates R and DrA and noncleavable substrate analogues RdA and D. Multiple conformational forms of both ribozyme and substrate Rt are present in our reactions (Figure 3), although each migrates as a single band in a denaturing gel (Figures 2A and 4). When individual species were eluted from native gels, heated, and renatured, the same banding pattern was obtained (data not shown). We believe that the lower mobility ribozyme species is either a catalytically inactive dimer or an inactive monomeric conformer. The higher mobility species is capable of binding substrate, while no binding of substrate or analogues to the more slowly migrating species was detected. This indicates that the higher mobility species is the active form of the ribozyme. Further evidence that the higher mobility form of the ribozyme is the catalytically active species was obtained. The variant ribozyme (Figure 1) migrates as a single band on native gels whose mobility exactly corresponds to that of the higher mobility ribozyme species in Figure 3 (data not shown).

Complexes between the ribozyme and substrate R and competitive inhibitor RdA are readily observed (Figure 3), and radiolabeled 5′ cleavage products are visualized. Complexes between ribozyme and the poorly cleaved substrate (DrA) and the noncleavable DNA analogue (D) were not observed under these conditions, demonstrating that the affinity of the ribozyme for DNA is much lower than for RNA and that binding is likely to be rate-limiting for DrA cleavage. Since ribozyme-catalyzed cleavage of DrA is observed (Figure 2A,B), we looked for complex formation under conditions of large ribozyme excess. Increasing amounts of a ribozyme·DrA complex were observed under conditions of 75-, 150-, and 300-fold molar excess of ribozyme (data not shown). Under identical conditions, complexes between the ribozyme and D were not observed. We have no evidence that the ribozyme binds D specifically. These findings indicate that the 2′-hydroxyl group of A_{-1} has two distinct functions—stabilization of the ribozyme–substrate complex and a direct role in catalysis. Our results demonstrate that ribose at A_{-1} contributes binding energy to the ribozyme–substrate complex and clearly indicate that other ribose moieties in the substrate contribute to binding as well. These data do not allow us to draw conclusions concerning the relative importance of individual ribose units.

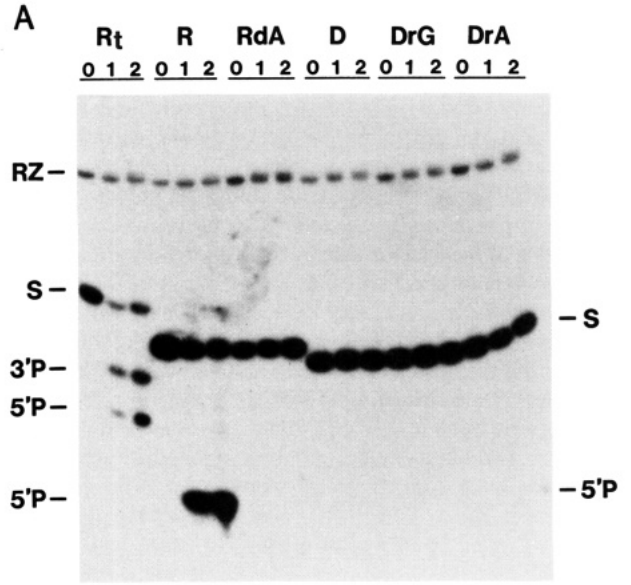

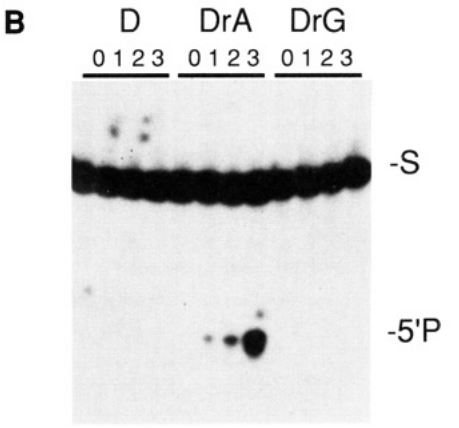

C

Substrate	KM (*nM*)	kcat (*min*$^{-1}$)	kcat/KM (*min*$^{-1}$*nM*$^{-1}$)	Relative Catalytic Efficiency
R	99 (±12)	1.3 (±0.2)	0.013	100
D	-	0	0	0
RdA	-	0	0	0
DrA	10,000 (±930)	0.060 (±0.003)	6.3×10^{-7}	0.0048
DrG	-	0	0	0

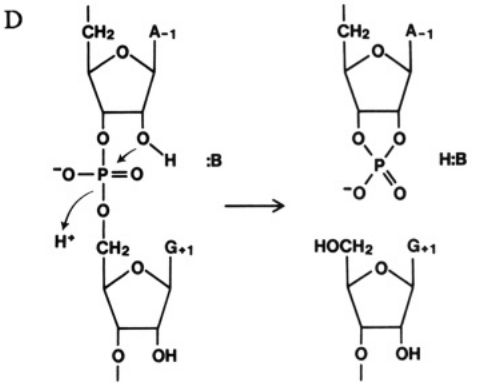

FIGURE 2: Cleavage of mixed RNA/DNA substrates by the hairpin ribozyme. (A) Cleavage assays. R, 14-base synthetic substrate RNA (see Figure 1 for sequence) Rt, 17-base substrate RNA synthesized by in vitro transcription. Sequence is that of R with 5′-terminal GCG added. RdA, 14-base synthetic substrate analogue with deoxyadenosine at position −1. D, 14-base synthetic DNA substrate analogue. DrG, substrate analogue consisting of DNA with a single riboguanosine at position +1. DrA, substrate analogue consisting of DNA with a single riboadenosine at position −1. RZ, ribozyme. S, substrate or substrate analogues. 3′P and 5′P, 3′ and 5′ cleavage products. 0, no $MgCl_2$. 1, 12 mM $MgCl_2$. 2, 100 mM $MgCl_2$. Ribozyme and substrate Rt were internally labeled with [α-^{32}P]CTP during transcription. Synthetic RNA and mixed RNA/DNA molecules were characterized by ribonuclease digestion and alkaline hydrolysis (data not shown), confirming the presence of deoxyadenosine at position −1 of RdA and riboadenosine at position −1 of DrA. The A_{-1}·G_{+1} linkage of DrA was cleaved to completion by ribonuclease T2. Reactions were terminated after 4 h (Rt and R) or 18 h (RdA, D, DrG, and DrA). Autoradiogram of a 20% polyacrylamide–urea gel is shown. Note that 3′ cleavage products of R and DrA are not visualized, since substrates are 5′-end-labeled. (B) Cleavage of substrate DrA at increasing ribozyme concentrations. To clearly demonstrate that RdA cleavage is ribozyme-catalyzed, we examined the effect of increasing ribozyme concentration. One picomole of end-labeled substrate was incubated with increasing quantities of unlabeled ribozyme (0, no ribozyme; 1, 75 pmol; 2, 150 pmol; 3, 300 pmol) in a 4-h reaction as described under Experimental Procedures (12 mM $MgCl_2$). The extent of DrA cleavage increased with ribozyme. No cleavage of substrate analogue RdA was observed under identical conditions (data not shown). (C) Kinetic parameters for substrates. Concentrations for R and DrA were 1–200 nM and 100 nM–10 μM, respectively. Ribozyme concentration was 1.8 nM. (D) Mechanism of cleavage. Results support cleavage via a transphosphorylation initiated by attack of the 2′-OH group of A_{-1} on the phosphorus in the A_{-1}·G_{+1} phosphodiester linkage.

The observation that the 2′-hydroxyl of A_{-1} is important for binding is consistent with the finding that K_d for inhibitor RdA (300 nM; unpublished results) is somewhat higher than K_M for substrate R (99 nM). At least two different mechanisms can explain the importance of ribose at position −1 in binding. The 2′-OH may directly interact with the ribozyme. Alternatively, replacement of ribose with deoxyribose may alter sugar conformation (i.e., 3′ endo to 2′ endo) and so destabilize the complex. Recent work has shown that the hammerhead ribozyme and *Tetrahymena* group I ribozyme also have a reduced affinity for a DNA substrate (Yang et al., 1990; Pyle et al., 1990), although in the latter case the DNA substrate is cleaved (Herschlag & Cech, 1990; Robertson & Joyce, 1990).

Why does the ribozyme bind a DNA substrate analogue so poorly? The 2′-OH groups of A_{-1} and other substrate residues may hydrogen-bond with functional groups of the ribozyme and so directly contribute to stabilization of the ribozyme–substrate complex. Alternatively, the altered conformation of the DNA–RNA heteroduplex (Wang et al., 1982; Walker, 1988; Chou et al., 1989) may interfere with binding by distorting the overall structure of the complex. Both of these factors may, in combination, result in the extremely poor binding of substrate DrA.

Substrate Selectivity and Alteration of Ribozyme Specificity. To test the kinetic effect of incorporating a phosphorothioate diester linkage at the cleavage site, it was necessary to create a variant ribozyme that cleaved a substrate with a single guanosine within the region recognized by the ribozyme (Figure 1). Cleavage activity of wild-type and variant ribozymes against cognate and mismatched substrates was analyzed (Figure 4A). Each ribozyme shows high activity and

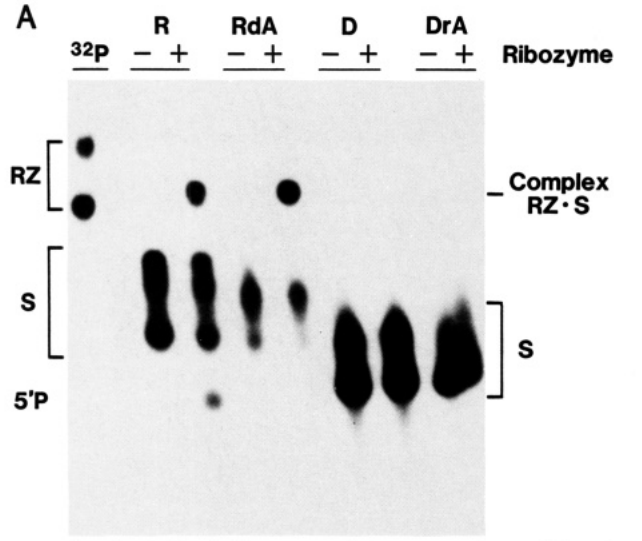

FIGURE 3: Analysis of ribozyme–substrate complexes. Complex formation was assayed by incubating renatured unlabeled ribozyme and ^{32}P-end-labeled substrate or substrate analogue in standard reaction buffer as described under Experimental Procedures. Gel analysis was carried out under identical conditions. In the leftmost lane, ribozyme is ^{32}P-labeled. Plus, ribozyme is present; minus, no ribozyme present.

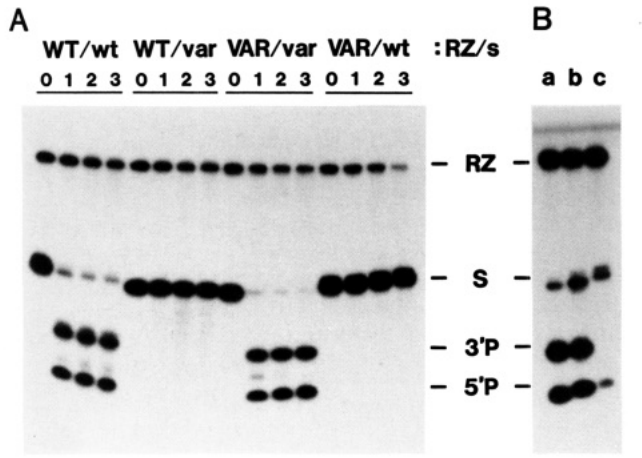

C

Ribozyme	Substrate	KM (*nM*)	kcat (min^{-1})	kcat/KM ($min^{-1}nM^{-1}$)
WT	wt(Rt)	43 (±4)	2.7 (±0.1)	0.063
VAR	var	37 (±8)	2.8 (±0.2)	0.076
VAR	var[αS]	45 (±5)	0.68 (±0.1)	0.015

FIGURE 4: Ribozyme activity against mismatched and phosphorothioate-substituted RNA substrates. (A) Sequence selectivity of the hairpin ribozyme. Wild-type and variant ribozymes and substrates (Figure 1) were transcribed and activity was analyzed as described for Figure 2. Reactions proceeded for 18 h. Uppercase, ribozyme; lowercase, substrate. $MgCl_2$ concentration was varied: 0, no $MgCl_2$; 1, 12 mM $MgCl_2$; 2, 50 mM $MgCl_2$; 3, 100 mM $MgCl_2$. (B) Cleavage of phosphorothioate linkage. Substrate containing a phosphorothioate at the cleavage site (Rt[αS]) was prepared by transcription as described above, except that α-phosphorothioate-substituted ribonucleoside triphosphates (NEN, 99.9% purity) were substituted as follows: lane a, no phosphorothioates; lane b, GTP[αS]; lane c, ATP[αS], UTP[αS], CTP[αS]. In lanes a and b substrates are labeled with α^{32}P-CTP. In lane c, substrate is labeled with [α-^{32}P]GTP. The 3′ cleavage product in lane c does not contain ^{32}P and so is not visualized. Reactions were for 60 min. (C) Kinetic parameters. The substrate and ribozyme concentrations were as described for the analysis of R cleavage (legend to Figure 2D).

specificity for cleavage of its cognate substrate. Single-base mismatches in helix 1 and helix 2 (C·C for wild type and G·G for the variant) are sufficient to eliminate cleavage activity. Kinetic analysis (Figure 4C) shows that activity of the variant ribozyme on its cognate substrate is kinetically indistinguishable from that of the wild type. This directly demonstrates that alteration of the cleavage specificity of the hairpin ribozyme can be accomplished without loss of catalytic efficiency.

Efficient Cleavage of Phosphorothioate. Kinetic analysis of the activity of the variant ribozyme against a substrate containing a single phosphorothioate at the cleavage site revealed no change in K_M and a 4-fold decrease in k_{cat} relative to hydrolysis of the phosphodiester linkage (Figure 4B,C). Single-burst kinetics were performed with a 4.2-fold molar excess of ribozyme over the substrate. Substrate was preloaded onto ribozyme as described in Figure 2; the reaction was initiated at 37 °C, and 10-μL aliquots were taken at several time points. The extent of cleavage was quantitated, the logarithm of the uncleaved fractions was plotted vs time, and first-order rate constants were determined (data not shown). Single-burst kinetics showed that the ratio of rates for the cleavage step (phosphate/phosphorothioate, k_O/k_S) was 1.5–2.0. It is clear that the ribozyme cleaves phosphorothioate linkages with high efficiency. Van Tol et al. (1990) showed that processing of (−)sTRSV transcripts proceeded when the transcripts were fully substituted with G[αS]. Although these experiments demonstrated that the ribozyme could cleave a phosphorothioate linkage, no conclusions could be drawn concerning the relative rates of cleavage for phosphorothioate vs phosphate.

The small decrease in rate at the cleavage step upon phosphorothioate substitution suggests that the *pro-*R_p (nonbridging) phosphoryl oxygen does not make an essential contact with Mg^{2+} in the ribozyme–substrate complex, since there is a strong preference for oxygen over sulfur in Mg^{2+} binding (Herschlag et al., 1991). The modest observed "thio effect" would be consistent with involvement of the *pro-*R_p oxygen in a tertiary interaction within the complex. Contrary to prevailing views, k_O/k_S ratios provide little information concerning rate-limiting steps of enzymatic RNA cleavage reactions, since k_O/k_S ratios of nonenzymatic reactions lie in the range of 1–4 (Herschlag et al., 1991; Burgers & Eckstein, 1979). These results are similar to those obtained for the *Tetrahymena* group I ribozyme (Herschlag et al., 1991) but very different from those seen for the hammerhead ribozyme, where incorporation of a single phosphorothioate at the cleavage site reduced the rate of cleavage to a much greater extent (Ruffner & Uhlenbeck, 1990). Detailed kinetic analysis will be needed to determine which step (substrate binding, substrate cleavage, product release, possible conformational change) is rate-limiting for the hairpin ribozyme.

ACKNOWLEDGMENTS

We thank Marty Fedor and Bob Cedergren for helpful comments on the manuscript and Tom Cech for comments and communication of results prior to publication.

REFERENCES

Burgers, P. M., & Eckstein, F. (1979) *Biochemistry 18*, 592–596.

Chou, S.-H., Flynn, P., & Reid, B. (1989) *Biochemistry 28*, 2435–2443.

Fedor, M. J., & Uhlenbeck, O. C. (1990) *Proc. Natl. Acad. Sci. U.S.A. 87*, 1668–1672.

Feldstein, P. A., Buzayan, J. M., & Bruening, G. (1989) *Gene 82*, 53–61.
Hampel, A., & Tritz, R. (1989) *Biochemistry 28*, 4929–4933.
Hampel, A., Tritz, R., Hicks, M., & Cruz, P. (1990) *Nucleic Acids Res. 18*, 299–304.
Haseloff, J., & Gerlach, W. L. (1989) *Gene 82*, 43–52.
Herschlag, D., & Cech, T. R. (1990) *Nature 344*, 405–409.
Herschlag, D., Piccarilli, J. A., & Cech, T. R. (1991) *Biochemistry 30*, 4844–4854.
McSwiggen, J. A., & Cech, T. R. (1989) *Science 244*, 679–683.
Milligan, J. F., & Uhlenbeck, O. C. (1989) *Methods Enzymol. 180*, 51–62.
Pyle, A. M., McSwiggen, J. A., & Cech, T. R. (1990) *Proc. Natl. Acad. Sci. U.S.A. 87*, 8187–8191.
Robertson, D. L., & Joyce, G. F. (1990) *Nature 344*, 467–468.
Rubino, L., Tousignant, M. E., Steger, G., & Kaper, J. M. (1990) *J. Gen. Virol. 71*, 1897–1903.
Ruffner, D. E., & Uhlenbeck, O. C. (1990) *Nucleic Acids Res. 18*, 6025–6029.
Ruffner, D. E., Dahm, S. C., & Uhlenbeck, O. C. (1989) *Gene 82*, 31–41.
Scaringe, S. A., Francklyn, C., & Usman, N. (1990) *Nucleic Acids Res. 18*, 5433–5441.
Van Tol, H., Buzayan, J. M., Feldstein, P. A., Eckstein, F., & Bruening, G. (1990) *Nucleic Acids Res. 18*, 1971–1975.
Walker, G. T. (1988) *Nucleic Acids Res. 16*, 3091–3099.
Wang, A. H.-J., Fujii, S., van Boom, J. H., van der Marel, G. A., van Boekel, S. A. A., & Rich, A. (1982) *Nature 299*, 601–604.
Yang, J., Perreault, J.-P., Labuda, D., Usman, N., & Cedergren, R. (1990) *Biochemistry 29*, 11156–11160.

Articles

Electron Transfer within Xanthine Oxidase: A Solvent Kinetic Isotope Effect Study†

Russ Hille

Department of Medical Biochemistry, The Ohio State University, Columbus, Ohio 43210

Received April 8, 1991; Revised Manuscript Received May 31, 1991

ABSTRACT: Solvent kinetic isotope effect studies of electron transfer within xanthine oxidase have been performed, using a stopped-flow pH-jump technique to perturb the distribution of reducing equivalents within partially reduced enzyme and follow the kinetics of reequilibration spectrophotometrically. It is found that the rate constant for electron transfer between the flavin and one of the iron–sulfur centers of the enzyme observed when the pH is jumped from 10 to 6 decreases from 173 to 25 s^{-1} on going from H_2O to D_2O, giving an observed solvent kinetic isotope effect of 6.9. An effect of comparable magnitude is observed for the pH jump in the opposite direction, the rate constant decreasing from 395 to 56 s^{-1}. The solvent kinetic isotope effect on k_{obs} is found to be directly proportional to the mole fraction of D_2O in the reaction mix for the pH jump in each direction, consistent with the effect arising from a single exchangeable proton. Calculations of the microscopic rate constants for electron transfer between the flavin and the iron–sulfur center indicate that the intrinsic solvent kinetic isotope effect for electron transfer from the neutral flavin semiquinone to the iron–sulfur center designated Fe/S I is substantially greater than for electron transfer in the opposite direction and that the observed solvent kinetic isotope effect is a weighted average of the intrinsic isotope effects for the forward and reverse microscopic electron-transfer steps. In both H_2O and D_2O the preponderance of the kinetic effect of a change in the thermodynamic driving force for the intramolecular electron-transfer reaction is on the microscopic rate constant for electron transfer from the flavin semiquinone to the iron–sulfur center. The results emphasize the importance of prototropic equilibria in the kinetic as well as thermodynamic behavior of xanthine oxidase and indicate that protonation/deprotonation of the isoalloxazine ring is concomitant with electron transfer in the xanthine oxidase system.

Xanthine oxidase is a complex metalloflavoprotein containing a molybdenum center, two 2Fe/2S centers of the spinach ferredoxin variety, and flavin adenine dinucleotide in each of its two identical and independent subunits (Hille & Massey, 1985; Bray, 1988). The reductive half-reaction of the catalytic cycle (xanthine hydroxylation to form uric acid) takes place at the molybdenum center of the enzyme (Bray et al., 1964), and the oxidative half-reaction (dioxygen reduction to peroxide or superoxide, depending on the level of enzyme reduction; Hille & Massey, 1981; Porras et al., 1981) at the FAD (Komai et al., 1965). Intramolecular electron transfer from the molybdenum to the FAD is thus an integral aspect of catalysis, and the enzyme serves a useful system in which to examine biological electron transfer. The prevailing hypothesis describing the behavior of xanthine oxidase is the rapid equilibrium model proposed by Olson et al. (1974), the basic premise of which is that reducing equivalents in partially reduced xanthine oxidase distribute themselves among the four redox-active centers of the enzyme according to their relative

†This work was supported by a grant from the National Science Foundation (DMB 88-04421).

0006-2960/91/0430-8522$02.50/0